REVISTA INGENIERÍA SÍSMICA

NÚMERO ESPECIAL

Resiliencia Sísmica de Edificaciones e Infraestructura

El presente artículo forma parte del Número Especial de la Revista Ingeniería Sísmica (RIS), publicado por la Sociedad Mexicana de Ingeniería Sísmica (SMIS), dedicado a diversos aspectos relacionados con la resiliencia sísmica de edificaciones e infraestructura.

SEISMIC VULNERABILITY ASSESSMENT OF A SCHOOL BUILDING WITH A COMMON STRUCTURAL TYPOLOGY IN AREQUIPA, PERU

David M. Chalco Pari(1,*), **Miguel A. Salas-Chávez**(1), and **Esteban M. Cabrera-Vélez**(2)

(1,*) Departamento de Arquitectura e Ingenierías de la Construcción, Universidad Católica San Pablo, Arequipa (Perú). dmchalco@ucsp.edu.pe. **Autor para correspondencia**

(1) Departamento de Arquitectura e Ingenierías de la Construcción, Universidad Católica San Pablo, Arequipa (Perú). miguelsalasc5@gmail.com

(2) Universidad del Azuay. Escuela de Ingeniería Civil / Instituto de Estudios de Régimen Seccional del Ecuador (IERSE), Cuenca (Ecuador). ecabrerav@uazuay.edu.ec

Número Especial desarrollado con la colaboración del Colegio de Ingenieros Civiles de México, A.C. y la Sociedad Mexicana de Ingeniería Sísmica

SEISMIC VULNERABILITY ASSESSMENT OF A SCHOOL BUILDING WITH A COMMON STRUCTURAL TYPOLOGY IN AREQUIPA, PERU

David M. Chalco Pari[(1,*)], *Miguel A. Salas-Chávez*[(1)], *and Esteban M. Cabrera-Vélez*[(2)]

ABSTRACT

Arequipa, located in southern Peru, is a region characterized by the frequent occurrence of earthquakes due to its proximity to the subduction interface between the Nazca and the South American plates. Consequently, school buildings in Peru are classified as essential facilities and are expected to remain operational after a severe earthquake. In this context, the seismic vulnerability assessment of public-school buildings is of critical importance, especially when a widely used structural typology, *Módulo 780-POST*, has been identified in several of these buildings. This study presents the seismic vulnerability assessment of a representative school building of this typology through nonlinear static (pushover) analysis, from which capacity curves were obtained in the main structural directions, and by evaluating and comparing the results of three different assessment frameworks: Vision 2000, Risk-UE and Hazus. The results reveal a clear direction-dependent vulnerability of the structure. In the most unfavorable direction, the structure reaches *Life Safety* performance level according to Vision 2000 and a *Moderate* damage state according to Risk-UE and Hazus. The corresponding mean global damage index is 46.67%, while the structural damage index reaches 24%. These findings highlight the implications of mixed structural systems on the seismic vulnerability of essential facilities and the importance of framework-dependent interpretation in vulnerability assessments.

Keywords: Seismic vulnerability; fragility; seismic risk; school building

ISSN-e 2395-8251

EVALUACIÓN DE LA VULNERABILIDAD SÍSMICA DE UN EDIFICIO ESCOLAR CON UNA TIPOLOGIA STRUCTURAL COMÚN EN AREQUIPA, PERÚ

RESUMEN

Arequipa, situada en el sur de Perú, es una región caracterizada por la frecuente ocurrencia de terremotos debido a su proximidad a la interfaz de subducción entre las placas de Nazca y Sudamérica. En consecuencia, los edificios escolares en Perú están clasificados como edificaciones

Artículo recibido el 13 de abril de 2026 y aprobado para su publicación el 28 de mayo de 2026. Se aceptarán comentarios y/o discusiones hasta cinco meses después de su publicación.

[(1,*)] Departamento de Arquitectura e Ingenierías de la Construcción, Universidad Católica San Pablo, Arequipa (Perú). dmchalco@ucsp.edu.pe.***Autor para correspondencia**

[(1)] Departamento de Arquitectura e Ingenierías de la Construcción, Universidad Católica San Pablo, Arequipa (Perú). miguelsalasc5@gmail.com

[(2)] Universidad del Azuay. Escuela de Ingeniería Civil / Instituto de Estudios de Régimen Seccional del Ecuador (IERSE), Cuenca (Ecuador). ecabrerav@uazuay.edu.ec

esenciales y se espera que se mantengan operativos tras un terremoto severo. En este contexto, la evaluación de la vulnerabilidad sísmica de los edificios escolares públicos es de importancia crítica, especialmente cuando se ha identificado una tipología estructural ampliamente utilizada, *el Módulo 780-POST*, en varios de estos edificios. Este estudio presenta la evaluación de la vulnerabilidad sísmica de un edificio escolar representativo de esta tipología mediante análisis estático no lineal (pushover), a partir del cual se obtuvieron curvas de capacidad en las principales direcciones estructurales, y mediante la evaluación y comparación de los resultados de tres marcos de evaluación diferentes: Visión 2000, Risk-UE y Hazus. Los resultados revelan una clara vulnerabilidad de la estructura dependiente de la dirección. En la dirección más desfavorable, la estructura alcanza un nivel de desempeño de *Seguridad de Vida* según Visión 2000 y un estado de daño *Moderado* según Risk-UE y Hazus. El índice de daño global medio correspondiente es del 46.67%, mientras que el índice de daño estructural alcanza el 24%. Estos hallazgos resaltan las implicaciones de los sistemas estructurales mixtos sobre la vulnerabilidad sísmica de edificaciones esenciales y la importancia de la interpretación dependiente del marco de trabajo en las evaluaciones de vulnerabilidad.

Palabras clave: Vulnerabilidad sísmica; fragilidad; riesgo sísmico; edificio escolar

ISSN-e 2395-8251

INTRODUCTION

Arequipa, located in southern Peru, one of the most seismically active zones of the world, has experienced several severe earthquakes. One of the last was the southern Peru earthquake that occurred on June 23, 2001, with a magnitude of 8.4 Mw (Hayes, et al. 2017) and a Mercalli Modified intensity of VII-VIII (Tavera, et al. 2001). According to INDECI (2002) in the region of Arequipa and its eight provinces, the earthquake caused 41 fatalities, 2,002 people injured, 15,751 homes affected, and 9,143 homes destroyed, and only in the homonymous province of the region, Arequipa, 219 educational facilities were affected and 587 were destroyed. Additionally, educational buildings (including school buildings) are categorized as essential facilities according to the Peruvian Seismic Design Code (SDC), formally designated *Norma Técnica E.030* in Spanish (SENCICO 2020), which must continue operating after a severe earthquake. It is essential to highlight the importance of these buildings performing in accordance with their design requirements.

A variety of methods are currently available for seismic vulnerability assessment, among which analytical approaches have been shown to provide greater accuracy (Kassem, Nazri and Farsangi 2020). Studies addressing the seismic vulnerability of educational buildings in Arequipa remain limited, and the present work is among the first to analytically assess the vulnerability of this building typology in the region. This study investigates an existing public-school building in Arequipa representative of the widely used *Módulo 780-POST* typology, with the objective of evaluating its seismic vulnerability through a comparison of three different assessment frameworks. This comparative study aims to highlight the need to complement multiple criteria to achieve a comprehensive interpretation of vulnerability results. In addition, the findings may support local authorities in the development of seismic risk assessment and mitigation strategies for school buildings of this typology.

SCHOOL BUILDING OF STUDY

This study focuses on a typical school building in Peru. The building is one of the seven blocks conforming to the government school named I.E. 40055 Romero Luna Victoria, located in the district of Cerro Colorado, in the province and region of Arequipa, Peru. Views of the building are presented in Figure 1; as shown in Figure 1(b), a one-story provisional structure is located adjacent to the school building and is not structurally connected to it. The three-story building has an overall plan dimension of 25.0 m in length and 8.45 m in width, with a typical floor height of 3.40 m. Based on the as-built drawings, the typical architectural floor plan and structural framing plan are presented in Figure 2.

The study building corresponds to a common structural typology in Peru known as *"Módulo 780-POST"* or *"modern Módulo 780"*. It consists of two- or three-story buildings with three classrooms per story (see Figure 2(a)). The designation *780* refers to the approximate plan dimensions of each classroom (about 7.80 m). The term *POST* indicates that these buildings were designed and built after 1997 in accordance with the 1997 Peruvian Seismic Design Code (SDC). In contrast, the *Módulo 780-PRE* typology refers to buildings constructed prior to 1997 and not designed under the 1997 Peruvian SDC. While the *780-PRE* and *780-POST* typologies are geometrically similar; the former typically incorporates weaker rectangular columns and commonly exhibits short-column effects due to the interaction with non-structural masonry partitions. Owing the increase on stiffness demands in the 1997 SDC, buildings of the *780-POST* typology have demonstrated improved seismic performance, as reported by Muñoz et al. (2004), who evaluated the responses of school buildings representative of both typologies. In addition, empirical fragility curves for these school buildings were proposed by Muñoz et al. (2007). For the present study, although the building was designed and built in 2011 under the 2003 Peruvian SDC, the *Módulo 780-POST* typology was retained.

ISSN-e 2395-8251

(a) (b)

Figure 1. (a) Frontal and (b) lateral elevation views of the school building under study

The *Módulo 780-POST* structural typology consists of a mixed structural system. In the X-direction, confined masonry walls are present along selected axes and alternate with reinforced concrete (RC) moment-resisting frames along the remaining axes. In contrast, the structural system in the Y-direction consists exclusively of RC moment-resisting frames (see Figure 2(b)). The confined masonry walls are located along axes 1, 3, 5, and 7 and are confined by horizontal RC tie-beams (V-102) and vertical RC tie-columns. Specifically, L-shaped tie-columns (C3) are provided along axes 1 and 7, while T-shaped tie-columns (C1) are used along axes 3 and 5. Each confined masonry wall is further composed of two masonry panels separated by an intermediate RC tie-column (C2). The cross-sectional dimensions and reinforcement detailing of the RC elements are illustrated in Figure 3. The floor and roof system consist of lightened one-way ribbed RC slabs with a total thickness of 200 mm. The ribs are oriented along the Y-direction, and the voids between ribs are filled with a clay brick of dimensions 300 mm × 300 mm × 150 mm, which are commonly used in Peru for short-span floor systems. The slab reinforcement comprises 1ϕ1/2" and 1ϕ3/8" bars as positive moment reinforcement at the bottom of each rib, and 2ϕ1/2" bars as negative moment reinforcement at the top of each rib. The RC slabs were cast in-situ and monolithically with the tie-beams and frame beams. The foundations supporting the confined masonry walls consist of continuous strip footings constructed of cyclopean concrete, with a depth of 1.30 m and a width of 1.15 m. A plain concrete plinth beam, matching the wall thickness, was constructed at the top of each strip footing. In addition, the frame columns and tie-columns are supported by RC isolated footings with plan dimensions of 2.00 m × 1.50 m and a depth of 0.60 m.

The masonry walls have a thickness of 250 mm and were constructed using locally manufactured industrial perforated clay bricks, commonly referred as *King Kong* masonry units, with nominal dimensions of 130 mm × 240 mm × 90 mm, using a cement-sand mortar with a mix proportion of 1:4. According to the design specifications, the compressive strength of the masonry is 6.374 MPa (65.0 kgf/cm^2). Based on the Peruvian Masonry Design Code, the corresponding modulus of elasticity is calculated as E_m=$500\sqrt{f_m'}$ [kgf/cm^2]= 32,500 kgf/cm^2 (3,187 MPa). The RC elements were constructed using normal-weight concrete with a specified cylindrical compressive strength of 20.59 MPa (210 kgf/cm^2). In accordance with the Peruvian Concrete Design Code, the elastic modulus of concrete is taken as E_c=$15000\sqrt{f_c'}$ [kgf/cm^2]= 217,371 kgf/cm^2 (21,317 MPa). Longitudinal and transverse reinforcement consist of ASTM A615 grade 60 deformed steel reinforcing bars, with a yield strength of 413.7 MPa (60 ksi) and an elastic modulus of E_s= 196,133 MPa (2.0 × 10^6 kgf/cm^2). The mechanical properties of all materials were obtained from the as-built drawings and are summarized in Table 1.

The building is in seismic zone 3 (of 4) according to the current Peruvian SDC (SENCICO 2020). The Peruvian code assigns a zone factor (Z) of 0.35 g, corresponding to the maximum horizontal ground acceleration in rigid soil for the design earthquake with a 10% probability of being exceeded in 50 years (a mean return period of 475 years). The site soil consists of a moderately stiff sand-gravel mixture and is classified as Type *"S_2"* according to the Peruvian SDC.

ISSN-e 2395-8251

ISSN-e 2395-8251

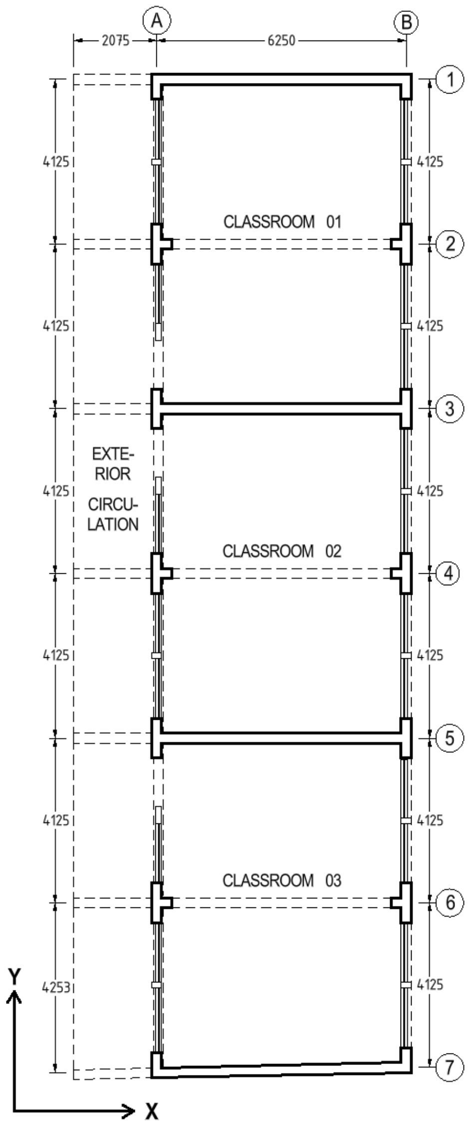

(a)

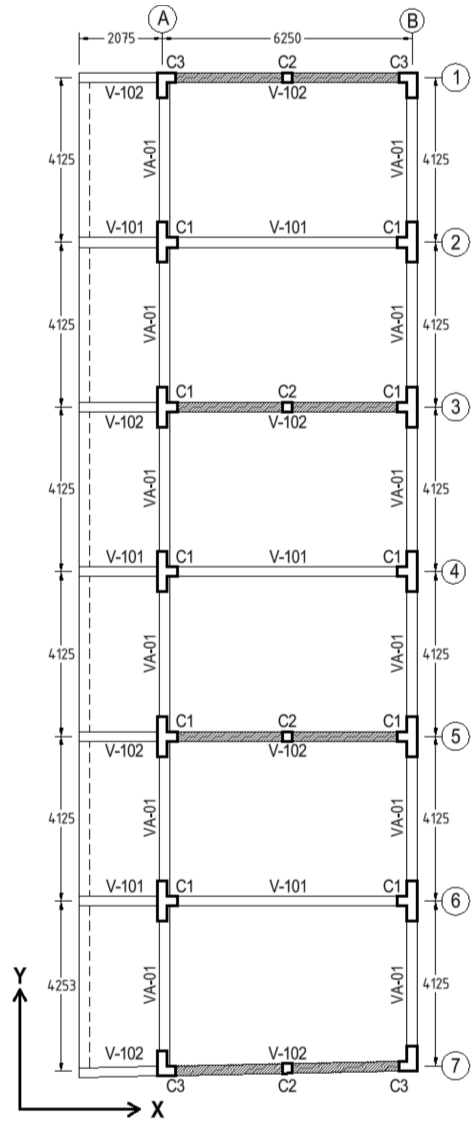

(b)

Figure 2. (a) Architectural floor plan, and (b) structural framing plan of the school building under study

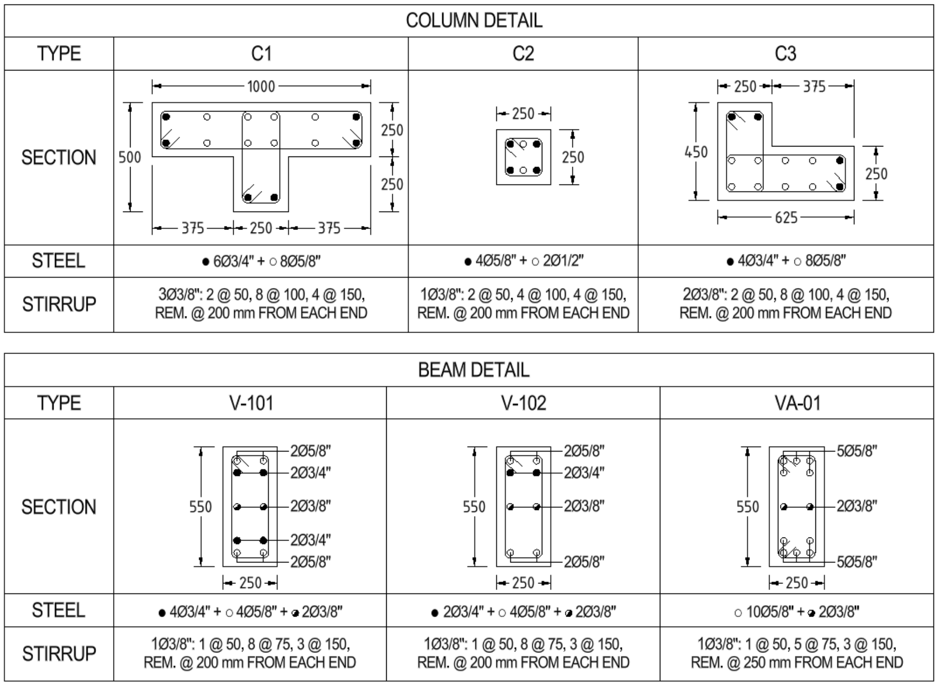

Figure 3. Cross-sectional dimensions and reinforcement detailing of RC columns and beams

Table 1. Mechanical properties of constituent materials

Material	Property	Value (MPa)
Concrete	Elastic modulus (E_c)	21,317
	Compressive strength (f_c')	20.59
Reinforcing steel	Elastic modulus (E_s)	196,133
	Yield strength (f_y)	413.7
Masonry	Elastic modulus (E_m)	3,187
	Compressive strength (f_m')	6.374

ISSN-e 2395-8251

NUMERICAL MODEL AND NONLINEAR STATIC ANALYSIS

The numerical model and nonlinear static analysis of the building were carried out by using the software ETABS (CSI 2022). The slabs were modeled using membrane elements, beams and columns using frame elements, and confined masonry walls using link elements. Plastic hinges definitions and yield rotations calculations were performed according to ASCE 41-13 specifications (ASCE/SEI 2013). The numerical model considers a rigid zone factor equal to 0.5 applied to frame elements (beams and columns). The reduction factors for inertia and shear area specified in ASCE 41-13 were used for each structural element. A three-dimensional view of the model is presented in Figure 4.

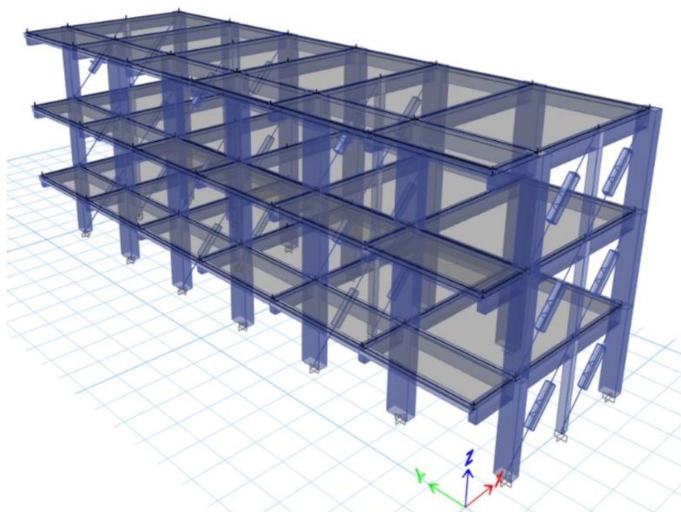

Figure 4. Three-dimensional view of the numerical model for the school building

ISSN-e 2395-8251

For the present study, the floor and roof slabs were modeled as rigid diaphragms and were assumed to remain elastic. This assumption was considered reasonable given the slab thickness, the absent of discontinuities in the lateral force-resisting system, their horizontal regularity, the presence of short-span bays, and a horizontal span-to-depth ratio less than 3; in accordance with the recommendations of the 2020 LATBSDC Alternative Analysis and Design Procedure (2020). In addition, soil-structure interaction was not considered in the structural analysis; therefore, the supports of the columns and walls were assumed to be fixed at the base.

The confined masonry walls were modeled using a macro-modelling approach based on the Equivalent Strut Model (ESM), originally proposed for RC frames with masonry infills. This approach was adopted under the assumption that failure modes of masonry infills and confined masonry walls are similar as demonstrated by Torrisi et al. (2012). In the present study the force-displacement relationship proposed by Panagiotakos and Fardis (1996) was employed, and nonlinear link elements were used in the analytical model to represent the confined masonry panels. Figure 5 illustrates the idealized trilinear force-displacement relationship for the most highly stressed confined masonry wall at the first story. The cracking point corresponds to a cracking shear strength of F_{cr} =543.3 kN at a displacement of d_{cr} =1.81 mm (0.05%), the maximum strength is reached at F_m =905.5 kN and d_m =5.70 mm (0.17%), while the residual strength is defined as F_r = 815 kN at a displacement of d_r =10.0 mm (0.29%).

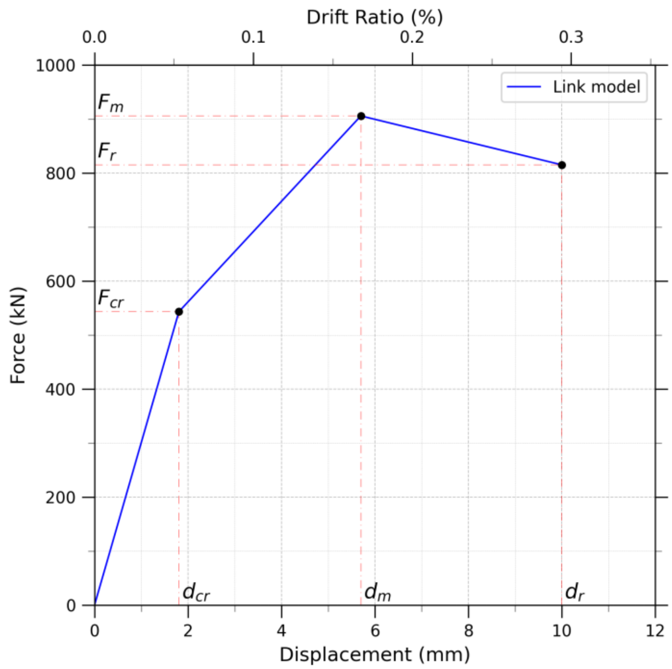

Figure 5. The force-displacement relationship for highly stressed confined masonry wall

ISSN-e 2395-8251

With the complete numerical model, a modal analysis was performed to obtain the period of the vibration modes and the modal participating mass ratios. The results are shown in Table 2.

Table 2. Periods and modal mass participation ratios per mode of school building

Mode	Period (s)	Cumulative modal participating mass ratios		
		Transl. in X	Transl. in Y	Rot. about Z
1	0.427	0	0.8051	0.0004
2	0.200	0.8833	0.8051	0.0004
3	0.182	0.8833	0.8053	0.8807
4	0.116	0.8833	0.9568	0.8807
5	0.071	0.9840	0.9568	0.8807
6	0.064	0.9840	0.9568	0.9838
7	0.057	0.9840	0.9995	0.9839
8	0.047	1	0.9995	0.9839
9	0.042	1	1	1

The nonlinear static analysis (ATC 1996, ATC 2005) was performed considering an increasing triangular lateral load pattern defined according to the Peruvian SDC (SENCICO 2020). This pattern is permitted by FEMA 440 (2005) and is widely used to approximate the first-mode-dominated response, as seen in Table 2, in regular low- to mid-rise buildings. During the analysis, special care was taken to ensure the convergence. The capacity curves for the considered school building in the X- and Y-direction are presented in Figure 6.

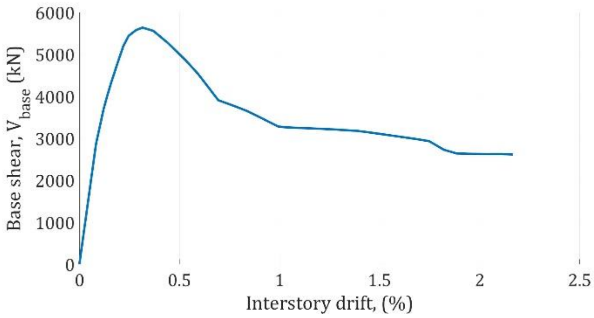

(a)

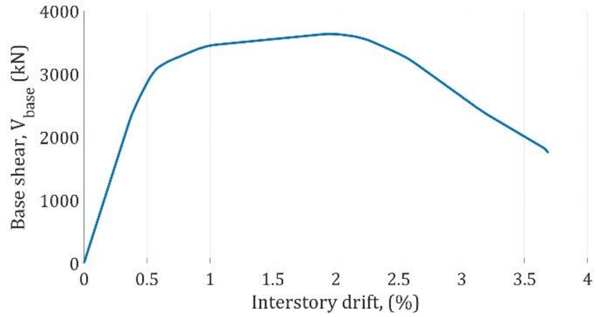

(b)

Figure 6. Capacity curves for the school building: a) X-direction, and b) Y-direction

Subsequently, the seismic demand obtained from the elastic design spectrum of the Peruvian SDC (Figure 7) is converted into the modified acceleration-displacement response spectrum (MADRS), which intersects the capacity curve at the performance point (PP) (ATC 2005). The PP represents the maximum displacement in a structure for a specific seismic demand. For this study, the PP is obtained by applying the improved equivalent linearization method procedure detailed in FEMA 440 (ATC 2005), which is an update of the capacity spectrum method presented in ATC-40 report (ATC 1996). The PP values obtained using this procedure are reported in Table 3. In this table, S_a denotes the spectral acceleration expressed as a fraction of the gravitational acceleration g, S_d represents the spectral displacement, D corresponds to the displacement of the control node located at the top story of the building, and V denotes the corresponding base shear force.

ISSN-e 2395-8251

Table 3. Performance points calculated according to FEMA 440 procedures for the school building

	S_a (g)	S_d (cm)	D (cm)	V (kN)
Dir. X	0.883	1.043	1.330	4321
Dir. Y	0.682	5.030	6.613	3246

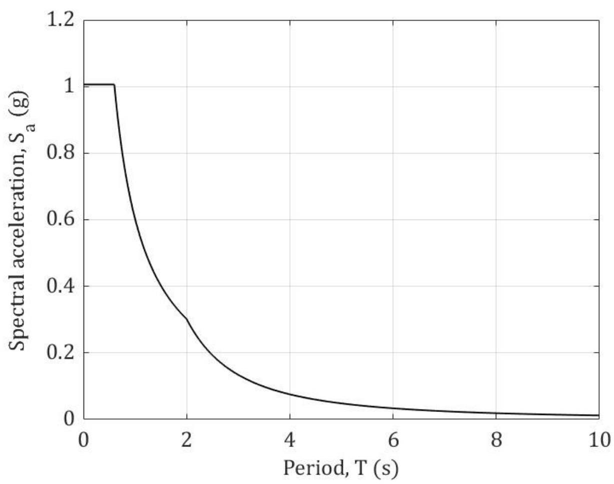

Figure 7. Elastic design response spectrum for Arequipa obtained from the Peruvian seismic design code for a 475-year mean return period earthquake

The plastic hinge patterns corresponding to the performance points for the X- and Y-direction are shown in Figure 8.

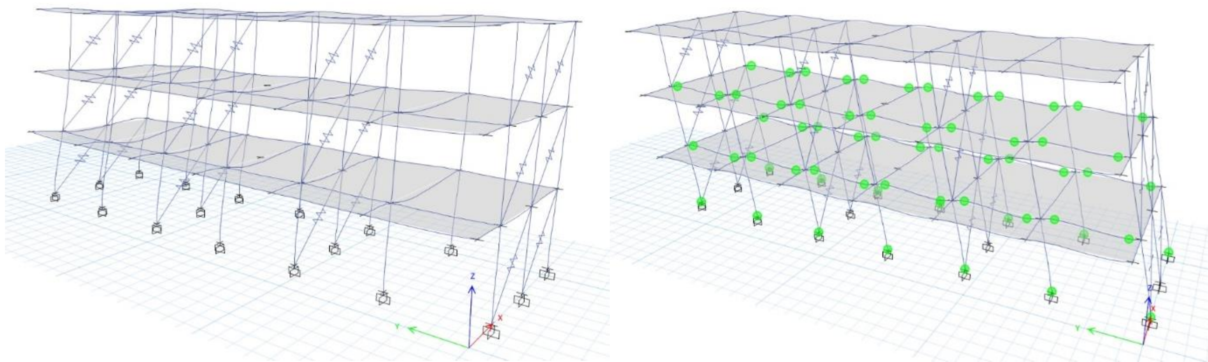

(a) (b)

Figure 8. Distribution of plastic hinges: a) X-direction, and b) Y-direction

Nonlinear static (pushover) analysis is a useful engineering tool for estimating global structural capacity an identifying plastic mechanism in structures whose response is dominated by the first mode, as is the case for the building examined in the present study. However, it cannot reliably capture higher-mode effects or dynamic characteristics; therefore, it should be complemented by nonlinear dynamic procedures, particularly when assessing irregular or high-rise structures.

ISSN-e 2395-8251

SEISMIC ASSESSMENT

The quantification of seismic vulnerability involves multiple sources of uncertainty. Therefore, to improve understanding and reduce uncertainty, three different vulnerability assessment frameworks -Vision 2000, Risk-UE, and Hazus- are evaluated and compared in this study. This comparative approach provides a more comprehensive characterization of the building's seismic vulnerability.

Performance level and damage state

A performance check is carried out using the performance limits defined according to Vision 2000 (SEAOC 1995), and the damage state is obtained according to the thresholds of damage states defined by Risk-UE (Milutinovic and Trendafiloski 2003) and Hazus (FEMA 2020). The results for the building can be seen in Figure 9., Figure 10, and Figure 11 respectively.

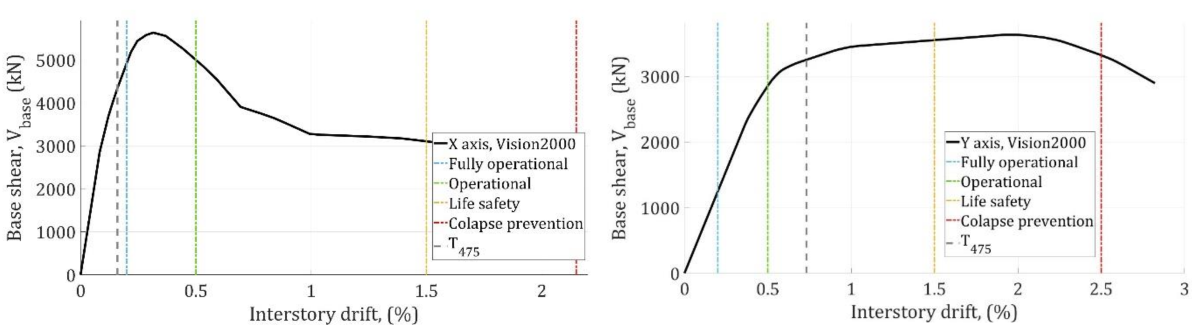

(a) (b)

Figure 9. Performance levels according to Vision 2000 for the building in (a) X-direction and (b) Y-direction respectively

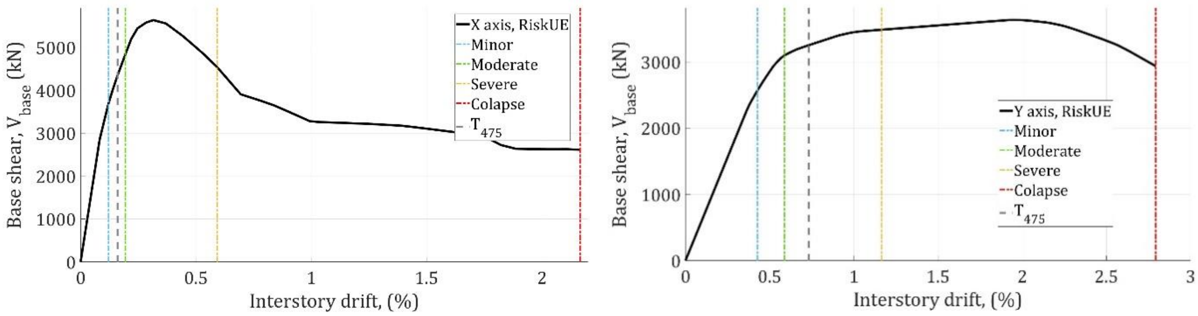

(a) (b)

Figure 10. Damage states according to Risk-UE for the building in (a) X-direction and (b) Y-direction respectively

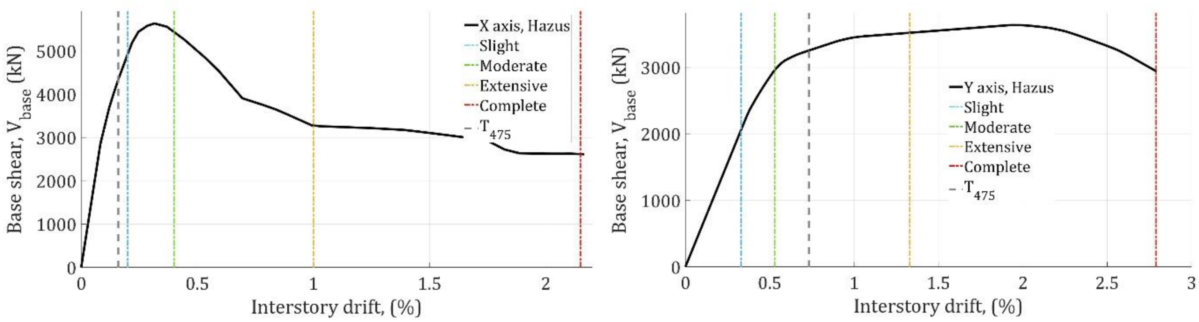

(a) (b)

Figure 11. Damage states according to Hazus for the building in (a) X-direction and (b) Y-direction respectively

ISSN-e 2395-8251

The graphics show that for the design earthquake with a 475-year mean return period, the structure in the X-direction is at the *Fully Operational* level according to Vision 2000 (SEAOC 1995) and in the damage states of *Minor* and *Slight* according to Risk-UE (Milutinovic and Trendafiloski 2003) and Hazus (FEMA 2020) respectively. In the Y-direction, for the same seismic demand, the structure is at the *Life Safety* level according to Vision 2000 and in the damage state of *Moderate* according to both Risk-UE and Hazus frameworks.

Fragility curves

Fragility curves allow us to establish, in terms of probability, the most probable damage state as a function of a selected intensity or demand parameter. In the present study, interstory drift -defined as the maximum relative lateral displacement between two adjacent floors normalized by the story height- is adopted as the governing parameter. This choice is motivated by the fact that the damage thresholds defined across the assessment frameworks considered are expressed in terms of interstory drift. Accordingly, this parameter is used to compare the structural response and the associated damage levels, thereby facilitating a consistent interpretation of the performance levels and damage states defined by each framework. A deep explanation of fragility curves can be seen in Barbat et al. (2008) and Vargas et al. (2013). The methodology to obtain fragility curves is established in documents as Risk-UE (Milutinovic and Trendafiloski 2003) and Hazus (FEMA 2020). Figure 12. presents the fragility curves obtained from the performance limits and damage states defined in the previous section in the same order as given in the last figures.

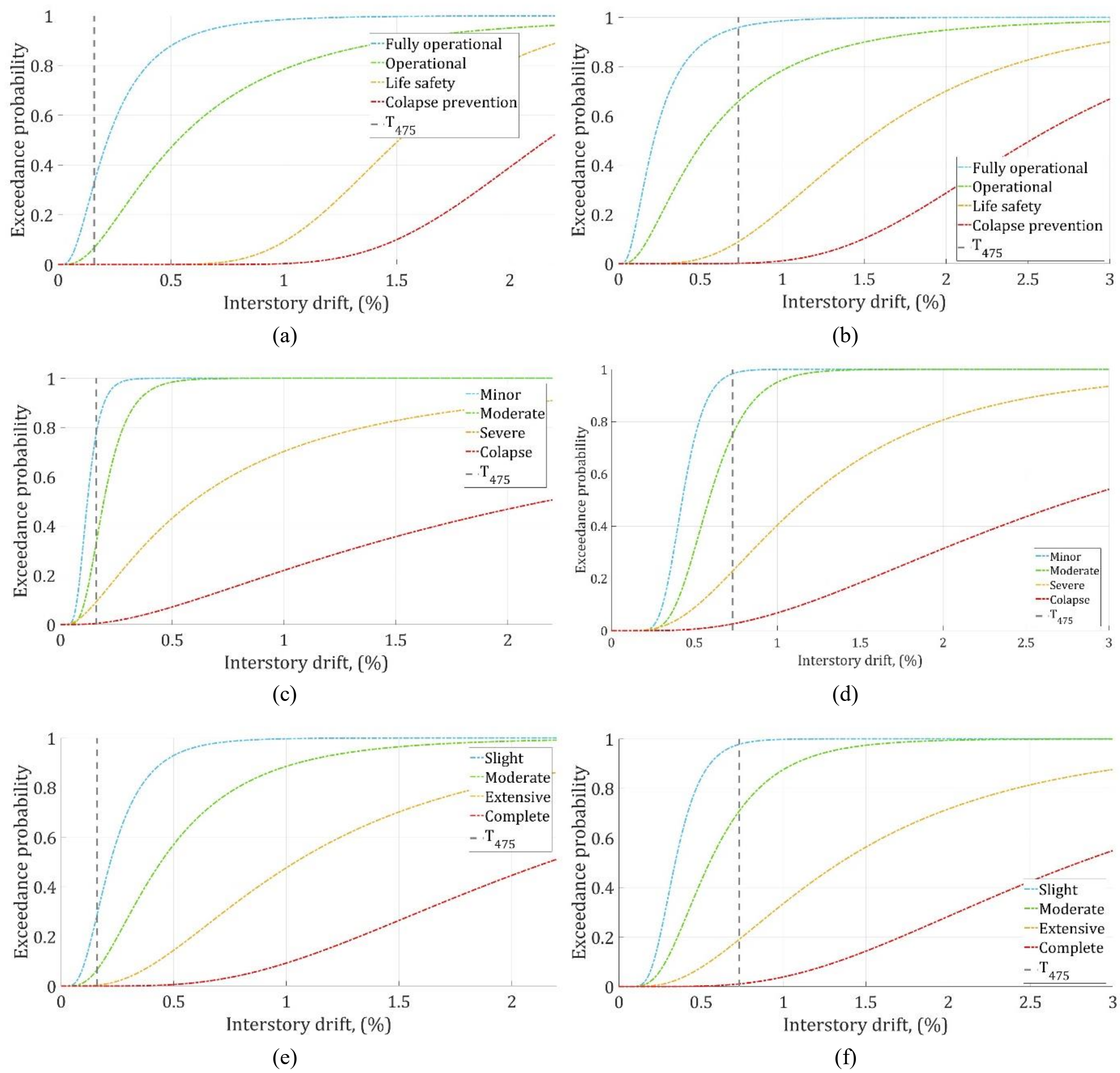

Figure 12. Fragility curves obtained from the performance limits according to Vision 2000, (a) and (b), and damage states according to Risk-UE, (c) and (d), and Hazus, (e) and (f), for the building in X-direction (left) and Y-direction (right) respectively

ISSN-e 2395-8251

Damage probability

From the fragility curves, vulnerability in terms of probability is obtained. Drawing the performance point obtained in the previous section on the fragility curves, the probability of being in or exceeding each of the different performance limits and damage states is obtained. Figure 13 presents the damage histograms, which show exceedance probabilities for each performance limit and damage state previously defined, as well as the most probable limit or damage state for the performance point in the X- and Y-direction.

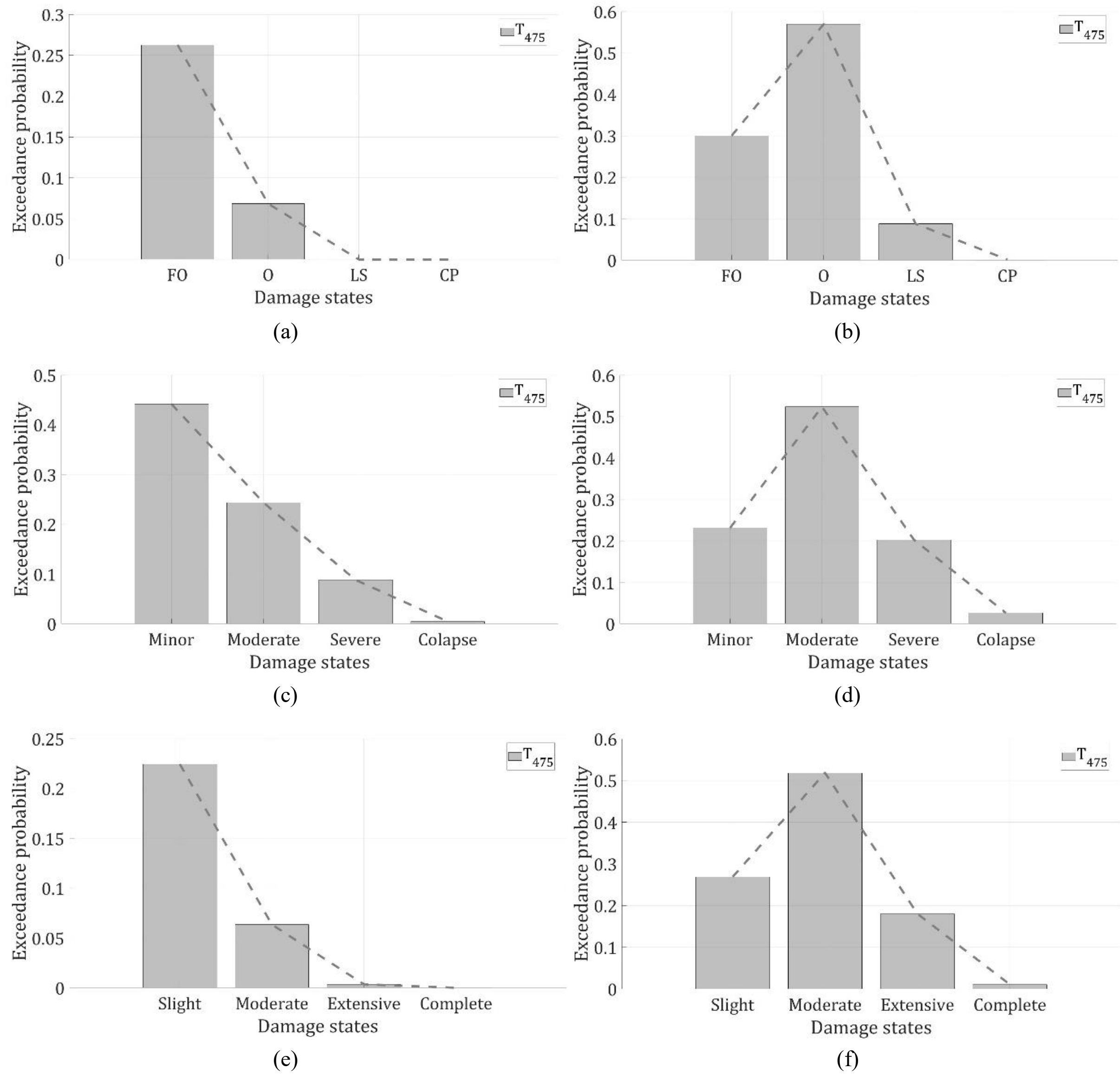

Figure 13. Damage probabilities obtained from the performance limits according to Vision 2000, (a) and (b), and damage states according to Risk-UE, (c) and (d), and Hazus, (e) and (f), for the building in X-direction (left) and Y-direction (right) respectively

For the X-direction, according to Vision 2000, the most probable performance level is *Fully Operational*, corresponding to minimal structural damage. According to Risk-UE and Hazus frameworks, the most probable damage states are *Minor* and *Slight* respectively, both associated with negligible to slight structural damage. For the Y-direction, according to Vision 2000, the most probable performance level is *Operational*, implying limited structural damage. Consistently, both Risk-UE and Hazus identify *Moderate* as the most probable damage state, characterized by slight structural damage and moderate non-structural damage.

ISSN-e 2395-8251

ISSN-e 2395-8251

Damage index

The vulnerability analysis concludes with the computation of a damage index, a quantitative parameter describing the level of damage on a scale from 0 to 1 (or 0% to 100%), where 0 indicates no damage and 1 indicates complete damage. In this study, two complementary criteria are employed to derive damage indices. The first criterion, proposed by Kappos (1997) and Kappos & Ellul (2000), defines a global damage index computed from fragility curves as a normalized weighted sum of the probabilities of exceedance of each damage state. This measure is hereafter referred to as the *global damage index*. The second criterion, proposed by Cabrera (2023), provides a damage index specifically associated with structural damage, which is derived from the performance point of the structure through the evaluation of the number of plastic hinges at each of the different damage levels, and is hereafter referred to as the *structural damage index*.

Based on the first criterion, Kappos, the global damage indices for each assessment framework and direction are presented in Figure 14. Correspondingly, the structural damage indices derived using the second criterion, Cabrera, are presented in Figure 15 for each framework and direction.

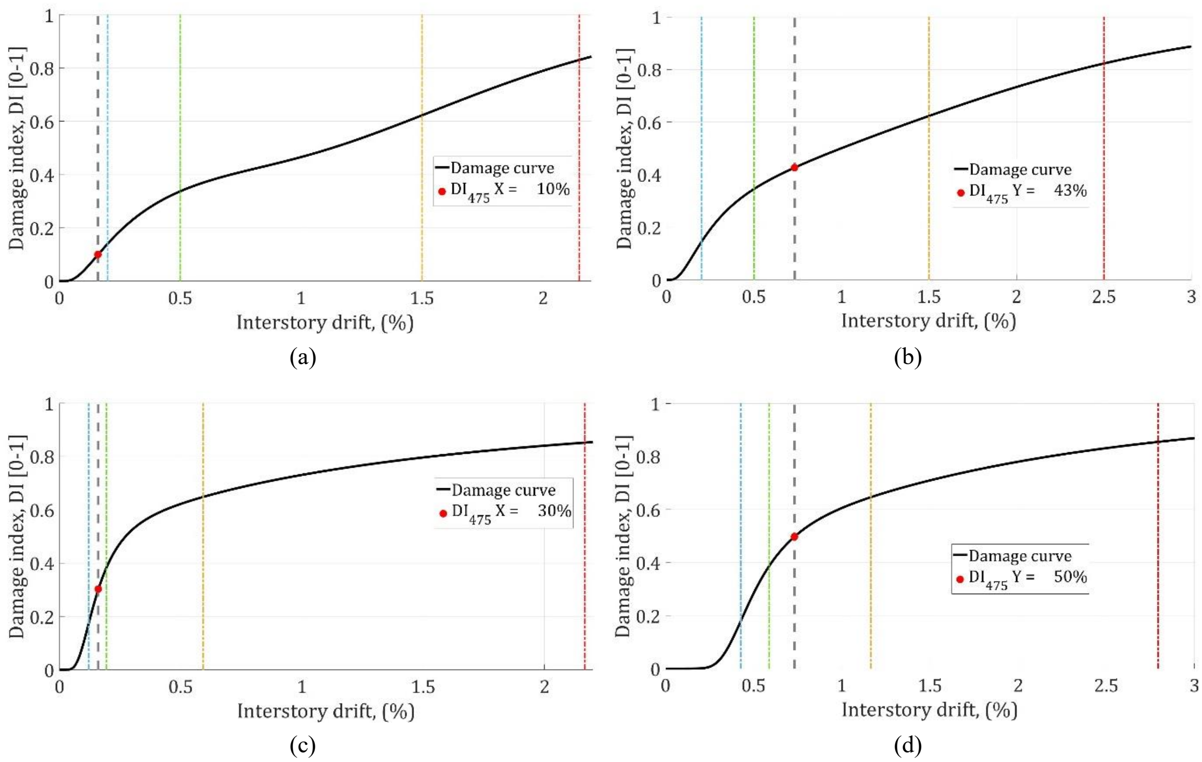

(a) (b) (c) (d)

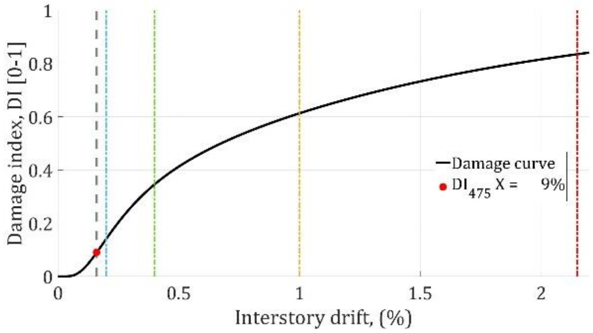

(e)

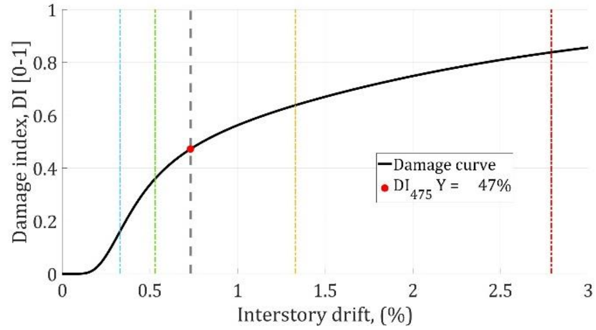

(f)

Figure 14. Damage curves and damage indices (DI) calculated according to the criteria of Kappos (1997), showing the performance limits according to Vision 2000, (a) and (b), and damage states according to Risk-UE, (c) and (d), and Hazus, (e) and (f), for the building in X-direction (left) and Y-direction (right) respectively

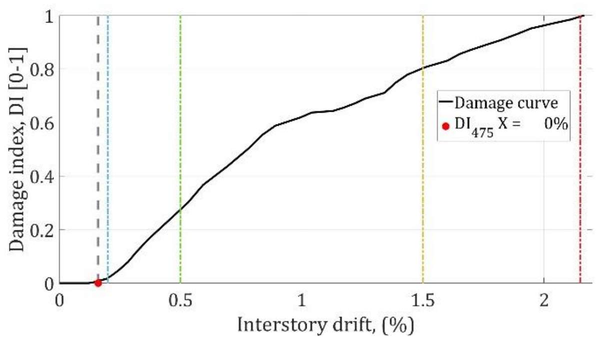

(a)

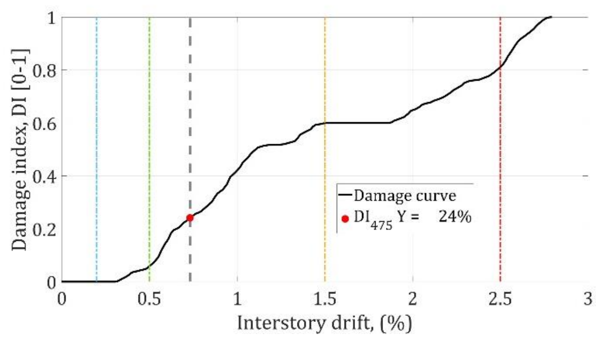

(b)

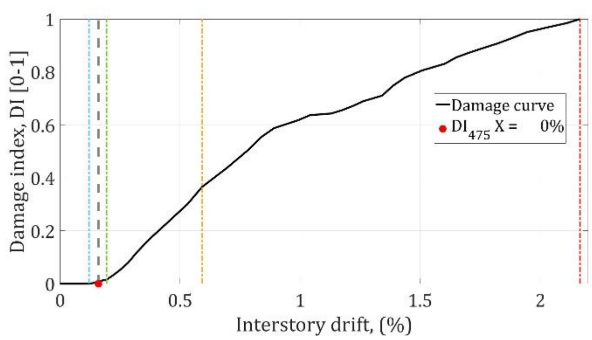

(c)

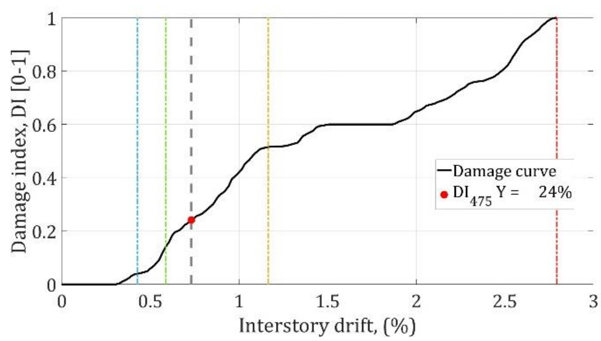

(d)

ISSN-e 2395-8251

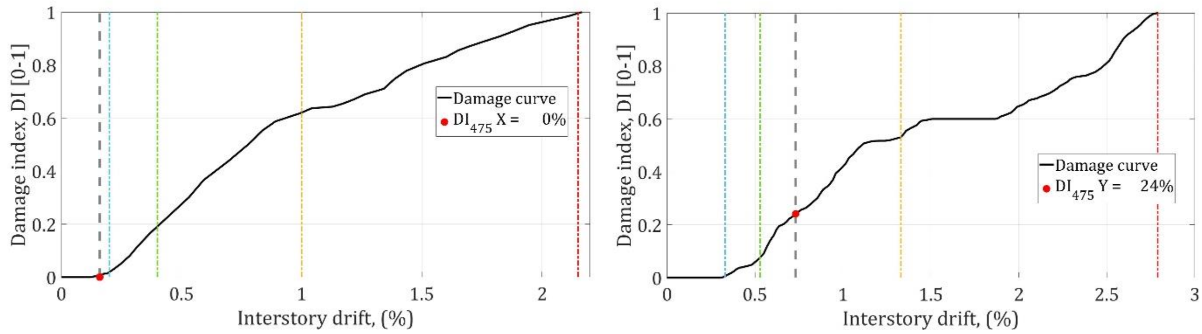

(e) (f)

Figure 15. Damage curves and damage indexes (DI) calculated according to the criteria of Cabrera (2023) locating the performance limits according to Vision 2000, (a) and (b), and damage states according to Risk-UE, (c) and (d), and Hazus, (e) and (f), for the building in X-direction (left) and Y-direction (right) respectively

The damage indices obtained according to the two criteria considered in this study are summarized in Table 4.

Table 4. Damage indices (DI) calculated according to Kappos (1997) and Cabrera (2023) criteria.

Criterion	Kappos – *DI* (%)		Cabrera- *DI* (%)	
	Dir. *X*	Dir. *Y*	Dir. *X*	Dir. *Y*
Vision 2000	10	43	0	24
Risk-UE	30	50	0	24
Hazus	9	47	0	24

ISSN-e 2395-8251

It is important to note that, according to Kappos' criterion, the structure presents a mean DI of 16.33% in the X-direction and a mean DI of 46.67% in the Y-direction. The DI=30% obtained by Risk-UE methodology is higher than the others. For the Y-direction, the associated damage is significantly higher, and although the structure may not collapse, the repair costs could be high. According to Cabrera's criterion for the X-direction, the structure presents no damage and a DI of 24% for the Y-direction.

The average or global damage index, proposed by Kappos, depends directly on the fragility curves. Therefore, the index calculated for each methodology changes. However, the index calculated from the performance point using the criterion proposed by Cabrera is the same, since the damage curve depends on the capacity curve. It is calculated based on the plasticization of structural elements for the displacement corresponding to the performance point. This index represents a direct relationship between the maximum displacement and the expected damage.

Regarding the above, a better approximation to the nonlinear behavior of a structure is obtained by considering as many criteria as possible. Each criterion describes the damage levels of the structure from different perspectives, and by complementing them, a better understanding is possible. These results could be improved if the numerical models are calibrated using ambient vibration measures (Gonzalez-Drigo, et al. 2019).

ISSN-e 2395-8251

DISCUSSION AND CONCLUSIONS

The nonlinear behavior of the school building is described by its capacity curves in each main direction of analysis, the curve in the X-direction describes a fragile behavior in comparison with curve in the Y-direction, this is because of the effect that the confined masonry walls have in X-direction. The maximum displacement, corresponding to the performance point, in X- and Y-direction are different, because the X-direction has great rigidity, but very reduced ductility. The structural system in the Y-direction is more ductile than in the X-direction.

The performance levels are acceptable in both main directions; however, the fragility-based results reveal a clear directional dependency. In the X-direction, the structure attains a *Fully Operational* performance level, with the most probable damage state classified as *Slight/Minor*. In contrast, in the Y-direction, *Life Safety* performance level, with *Moderate* damage identified as the most probable damage state. This directional discrepancy is further reflected in the damage indices, which are significantly higher in the Y-direction than in the X-direction The mean global damage index derived using the Kappos criterion is 16.33% for the X-direction and 46.67% for the Y-direction, whereas the structural damage index obtained using the Cabrera criterion is 0% and 24%, respectively. These differences arise from the distinct conceptual bases of the two approaches. While both criteria consistently identify the Y-direction as more vulnerable, the structural damage index is considered more representative of the actual structural response, as it is derived from the nonlinear analysis. Nevertheless, the combined use of indices provides a useful range of potential damage outcomes, offering a more comprehensive characterization of the building's seismic vulnerability.

The presence of a mixed structural system in the school building, that is, a different lateral force-resisting system for each main direction, poses a significant structural concern, as it leads to direction-dependent vulnerabilities. Consequently, this typology is not recommended, particularly for buildings classified as essential facilities, such as the school examined in this study. Based on a field survey conducted by the research team, it is estimated that approximately 50% of school buildings in Arequipa, Peru, exhibit this structural configuration. Given that the studied building corresponds to the widely used *Módulo 780-POST* typology across Peru, the findings of this research may assist local authorities in the development of informed seismic risk assessment and mitigation strategies for school buildings of this typology.

ACKNOWLEDGMENTS

This research was developed thanks to funding from the "25 years at the service of research of the Universidad Católica San Pablo" contest, project with reference UCSP-2022-25años-P21. The authors would also like to thank the support of the research program: "Structural health assessment in buildings applying advanced vulnerability analysis methodologies and RAR technology, Phase 2, and Phase 3" with codes 2024-0141 and 2025-0150 (IERSE, Universidad del Azuay).

REFERENCES

Alva, R E, E Cabrera Velez, R: Vargas-Alzate, Y F Gonzales-Drigo, L Pujades, J Avila-Haro, and G Luzi. 2024. "SEISMIC DAMAGE ASSESSMENT OF CONCRETE BUILDINGS INCLUDING THE CONTRIBUTION OF INFILL MASONRY WALLS." *18th World Conference on Earthquake Engineering.* Milan.

ASCE/SEI. 2013. *ASCE/SEI 41-13: seismic evaluation and retrofit of existing buildings.* Reston, Virginia: American Society of Civil Enginers - ASCE.

ATC. 1996. *ATC-40 Seismic Evaluation and Retrofit of Concrete Buildings. Volume 1. Report No. SSC 96-01.* Redwood City: Applied Technology Council - ATC.

ATC. 2005. *FEMA 440 Improvement of Nonlinear Static Seismic Analysis Procedures.* Redwood City: Applied Technology Council - ATC.

Barbat, Alex H, Luis G Pujades, and N Lantada. 2008. "Seismic damage evaluation in urban areas using the capacity spectrum method: Application to Barcelona." *Soil Dynamics and Earthquake Engineering* (28): 851-865.

Cabrera, E M. 2023. *Metodología para estimación del daño sísmico en edificios en base a modelos numéricos avanzados y monitorizaciones RAR.* Barcelona: Tesis doctoral, Universidad Politécnica de Cataluña. doi:10.5821/dissertation-2117-396558.

CSI. 2022. "ETABS building analysis and design v20.1.0." Computers and Structures, Inc. -CSI.

FEMA. 2020. *Hazus Earthquake Model Technical Manual. Hazus 4.2 SP3.* Federal Emergency Managment Agency - FEMA.

Gonzalez-Drigo, R, E. Cabrera, G Luzi, L G Pujades, Y F Vargas-Alzate, and J Avila-Haro. 2019. "Assessment of post-earthquake damaged building with interferometric real aperture radar." *Remote Sensing* 11 (23).

Hayes, G P, E K Myers, J W Dewey, R W Briggs, P S Earle, H M Benz, G M Smoczyk, et al. 2017. *Tectonic summaries of magnitude 7 and greater earthquakes from 2000 to 2015.* U.S. Geological Survey Open-File Report 2016–1192, 148. doi:https://doi.org/10.3133/ofr20161192.

INDECI. 2002. *Compendio Estadístico de Emergencias 2001.* Instituto Nacional de Defensa Civil, Lima: Instituto Nacional de Defensa Civil - INDECI, 350.

Kappos, A J. 1997. "Seismic damage indices for RC buildings: evaluation of concepts and procedures." *Progress in Structural Engineering and Materials* 1 (1): 78-87. doi:10.1002/pse.2260010113 .

Kappos, A J, and F Ellul. 2000. "Seismic design and performance assessment of masonry infilled R/C frames." *12th World Conference on Earthquake Engineering.* 1-8.

Kassem, M N, F M Nazri, and WE N Farsangi. 2020. "The seismic vulnerability assessment methodologies: A state-of-the-art review." *Ain Shams Engineering Journal* 11: 849-864.

Los Angeles Tall Buildings Structural Design Council. 2020. "An Alternative Procedure For Seismic Analysis And Design Of Tall Buildings Located In The Los Angeles Region."

Milutinovic, Zoran V, and Goran S Trendafiloski. 2003. "Risk-UE An advanced approach to earthquake risk scenarios with applications to different European towns. Contract: EVK4-CT-2000-00014. WP4: Vulnerability of current buildings." 110.

Muñoz, A., M. Blondet, R. Aguilar, and M.-A. Astorga. 2007. "Empirical Fragility Curves For Peruvian School Buildings." *Sixth International Conference on Earthquake Resistant Engineering Structures.*

Muñoz, A., M. Blondet, U. Quintana, and H. Leon. 2004. "Earthquake-Resistant Performance of Peruvian School Buildings." *13th World Conference on Earthquake Engineering.* Vancouver.

Panagiotakos, T B, and M N Fardis. 1996. "Seismic response of infilled RC frames structures. Paper No. 225." *Eleventh World Conference on Earthquake Engineering.*

Pujades, L G, Y F Vargas-Alzate, A H Barbat, and J R González-Drigo. 2015. "Parametric model for capacity curves." *Bulletin of earthquake engineering* 13: 1347-1376.

SEAOC. 1995. *Vision 2000: performance based seismic engineering of buildings.* Sacramento: Structural Engineers Association of California - SEAOC.

SENCICO. 2020. *Norma E.030 Diseño Sismorresistente.* Lima: Servicio Nacional de Capacitación para la Industria de la Construcción - SENCICO.

Tavera, Hernando, H Salas, C Jimenez, Y Antayhua, L Vilcapoma, J Millones, I Bernal, et al. 2001. *El terremoto de Arequipa del 23 de junio de 2001. Informe Preliminar.* Lima: IGP.

Torrisi, G. S., F. J. Crisafulli, and A. Pavese. 2012. "An innovative Model for the In-Plane Nonlinear Analysis of Confined Masonry and Infilled Frame Structures." *Fifteenth World Conference on Earthquake Engineering.* Lisbon.

Vargas, Y, L Pujades, A Barbat, and J Hurtado. 2013. "Evaluación probabilista de la capacidad, fragilidad y daño sísmico de edificios de hormigón armado." *Revista internacional de métodos numéricos para cálculo y diseño en ingeniería* 29 (2): 63-78.

ISSN-e 2395-8251